J Mol Model (2012) 18:4985–4993
DOI 10.1007/s00894-012-1498-9

ORIGINAL PAPER

Theoretical study on ion-pair recognition of M^+X^- (M = Li, Na, K and X = F, Cl, Br) by formylaminocalix[4] arene derivatives

Ju Xie · Guolian Jin · Long Sun · Wenling Feng · Pengfei Lu · Guowang Diao

Received: 19 June 2011 / Accepted: 7 June 2012 / Published online: 26 June 2012

Abstract DFT calculations were reported for calix[4] arene derivatives [*i.e.*, formylaminocalix[4]arene (**1**) and formylaminocalix[4]bis-crown-3 (**2**)] binding cations M^+ (Li^+, Na^+, and K^+) and anions X^- (F^-, Cl^-, and Br^-) simultaneously. The B3LYP function together with the LANL2DZp basis set was used in order to obtain insights into the factors determining the nature of the interactions of these compounds with X^- and M^+. Based on the molecular electrostatic potential (MEP) analysis, the result complexes M^+X^-/H (H=**1**, **2**) were investigated. For all the complex structures, the most pronounced changes in geometric parameters upon interaction were observed in the host segment compared with the free receptors. Two main types of driving force, N-H X^- hydrogen bonds and electrostatic interactions between M^+ and oxygen atoms, were confirmed. The recognition trends for **1** and **2** toward M^+X^- followed the same order: $M^+F^- > M^+Cl^- > M^+Br^-$ (M^+ is same to each other) and $Li^+X^- > Na^+X^- > K^+X^-$ (X^- is same to each other). The binding energy, enthalpy change, Gibbs free energy change, and entropy change of complexation formation have been studied by the calculated thermodynamic data. In all cases, the inclusion energy changes with **2** were more negative than those with **1**, correlating with the flexible space available by the two crown ether moieties in **2**. The calculated results of the model system have been reported and should be useful to the experimental research in this field.

J. Xie (✉) · G. Jin · L. Sun · W. Feng · P. Lu · G. Diao
College of Chemistry and Chemical Engineering,
Yangzhou University,
Yangzhou, China
e-mail: xieju@yzu.edu.cn

Keywords Calix[4]arene derivatives · Density functional theory (DFT) · Ion pair recognition · Supramolecular chemistry

Introduction

The design and application of new heteroditopic receptor systems capable of simultaneous coordination of both anionic and cationic guest species has recently attracted a great deal of interest, as these systems have the potential to act as salt solubilization, extraction, and membrane transport agents [1]. A number of receptors whereby an anion and cation are bound separately within the receptor have been reported previously [2–11]. In these systems, the cation may be bound using a number of common motifs including crown ethers, and π-electron donors, such as functionalized calixarenes, while the anion is coordinated using Lewis acidic, electrostatic, or hydrogen bonding interactions. In fact, in many cases, ion-pair receptors containing binding sites for both cations and anions display affinities for ion pairs or their constituent pairs of ions that are enhanced relative to simple ion receptors. In 2009, Secchi and coworkers described the ion pair receptors, where the upper rim of the cone-calix[4]arene moiety is covalently connected with an anion recognizing urea group through a methylene spacer [12]. These receptors display a binding ability that is enhanced by up to two orders of magnitude for organic salts with respect to the simple cation receptors. In the resulting complexes, the cations are bound to the electron-rich arene rings of the calix[4]arene moiety *via* cooperative C-H π and cation-π interactions, while the anions interact with the urea moiety *via* hydrogen bonds. By contrast, the monotopic receptors recognize these organic salts *via* only C-H π and cation-π interactions (*i.e.*, without the benefit of additional

anion-host interactions). Therefore, the development of ion-pair receptors is one of the most attractive fields of supramolecular chemistry.

Computational methods have significantly improved over the last years allowing now a better theoretical understanding of the features and binding properties of supramolecular recognition events [13–17]. In this work, two novel calix[4]arene derivatives, formylaminocalix[4]arene (**1**) and formylaminocalix[4]bis-crown-3 (**2**) (see Fig. 1), as ion-pair receptors have been designed. The relative binding affinities as well as binding sites and interaction modes of receptors **1** and **2** toward ion pairs M^+X^- (M = Li, Na, K and X = F, Cl, Br) were theoretically investigated using the density functional theory (DFT) method. The calculated results also provide the information toward the derivatization possibility, which would be of general interest to experimental chemists.

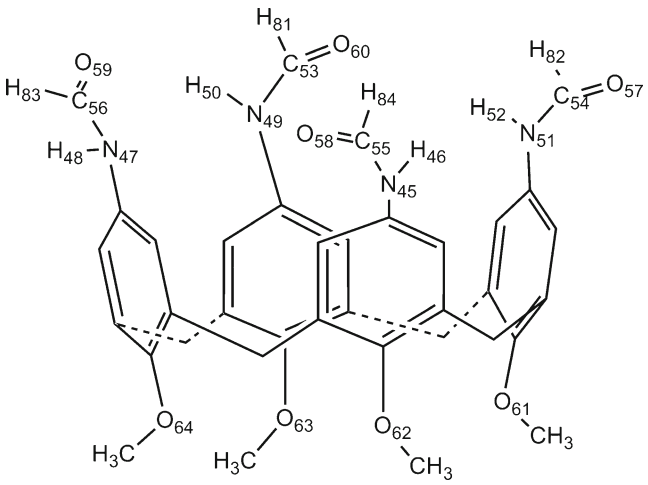

1

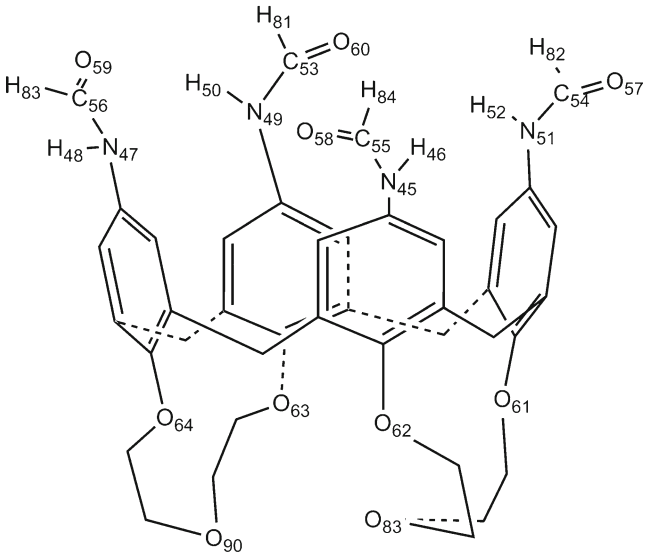

2

Fig. 1 Chemical structures of the used species in the cone conformation, formylaminocalix[4]arene (**1**) and formylaminocalix[4]bis-crown-3 (**2**)

Computational methods

The geometrical structures of formylaminocalix[4]arene (**1**), formylaminocalix[4]bis-crown-3 (**2**), and complexes, M^+X^-/H (M = Li, Na, K; X = F, Cl, Br; H=**1**, **2**) were fully optimized using the DFT methods at the LANL2DZp basis set with the exchange potential of Becke [18] and correlation functional of Lee, Yang, and Parr [19] (B3LYP). LANL2DZp basis set contains the standard LANL2DZ basis set including an additional set of polarization function [20–22]. The obtained interactional energies of the complexation were corrected for both basis set superposition error (BSSE) by the Boys-Bernardi full counterpoise method [23] and zero-point energy correction (ZPE). Harmonic vibrational frequencies and intensities were calculated both for free host and guest species and the complexes at 298.15 K. All calculations were performed by using Gaussian 09 program [24].

The complexation reaction for the calculation of thermodynamic properties were shown as follows:

$$H_{free} + M^+{}_{free} + X^-{}_{free} \rightarrow (M^+X^-/H)_{complex}. \quad (1)$$

Wherein H is receptor **1**, **2**; M is Li, Na, and K; X is F, Cl, and Br.

For this system, the binding energy ΔE can be expressed as follows:

$$\Delta E = E(M^+X^-/H)_{complex} - E(H)_{free} - E(M^+)_{free} - E(X^-)_{free} + E_{bsse}. \quad (2)$$

The Gibbs free energy change (ΔG) of the complexation reaction was given by

$$G = G(M^+X^-/H)_{complex} - G(H)_{free} - G(M^+)_{free} - G(X^-)_{free}. \quad (3)$$

Equation 3 was also used to calculate the changes in enthalpy (ΔH) and entropy (ΔS).

Results and discussion

Optimized geometry and electronic potential surface of receptors 1 and 2

Both the free calix[4]arene derivatives **1** and **2** are in cone conformations. The cone conformation has a cavity which

has inspired the use of calix[4]arene as host molecules and potential enzyme mimics. The obtained optimized geometries of **1** and **2** are shown in Fig. 2 with the selected most interesting geometrical parameters listed in Tables 1 and 2. As indicated by all the real frequencies, the optimized structures appear to be true minima. Inspection of Fig. 2, reveals that the optimized structure **1** is present in almost C_{2V} symmetry form. As to the substitutions of the calix[4]arene, both the upper side amide functions –NHC(O)H and the lower side methoxyl groups can perfectly overlap with the opposite ones. Furthermore, receptor **1** is found to adopt a pinched cone conformation, in which the distances of N45-N49 and N47-N51 are 5.233 Å and 12.105 Å, respectively. Accordingly, the distances for O62-O63 and O61-O64 are 5.720 Å and 3.395 Å, respectively, through the rigid phenyl group. Such a big distance difference is improved in receptor **2**, and the distances of N45-N49 and N47-N51 are 6.957 Å and 10.038 Å, respectively. In the host 2, there are two weak hydrogen bonds between neighbor N-H group and the carbonyl oxygen, the distances for H48 O58 and H52 O60 are 2.291 Å and 3.771 Å, respectively. These weak interactions may play an important role in stabilizing of structure 2. Due to the replacement of four methoxyl groups on the lower rim of **1** by two crown-3 subunits, the symmetry of **2** decreases slightly. Two crown ether loops are not perfectly overlapped with each other because of the electrostatic repulsion and spatial effect.

Molecular electrostatic potential (MEP) [25] has been found to be useful to explore molecular recognition, and a MEP analysis could reveal for a guest the preferential binding site in the host molecule [26, 27]. The MEP surfaces of receptors **1** and **2** have been generated from the Gaussian output files at the B3LYP/LANL2DZp level. The MEP (in a.u.) presented over electronic isodensity 0.005 electron/bohr^3 are illustrated in Fig. 3. As shown in Fig. 3, the electronic isodensity surfaces of **1** and **2** show the strongly positive values on the hydrogen atom of the amide group –NHC(O)H at the wide upper rim of calix[4]arene with intense blue, where **1** and **2** would be preferentially attacked by nucleophilic reagents. The negative MEP values are mainly from two kinds of oxygen atoms with red color, the oxygen atom of the amide group and the oxygen atom of the phenolic group in **1** and the crown ether subunit in **2** at the narrow lower rim of calix[4]arene, where the electrophilic reagents could interact with the receptors. Based on the MEP results, it is presumed that the receptors **1** and **2** could bind the anion X^- of ion-pair M^+X^- by the amide group at the wide upper rim and the cation M^+ at the narrow lower rim of calix[4]arene moiety.

Optimized geometries of complexes

The optimized representative structures of the complexes, M^+X^-/H (M = Li, Na, K; X = F, Cl, Br; H=**1**, **2**) are shown in Fig. 4, and the most relevant parameters for M^+X^-/H optimized at B3LYP/LANL2DZp level are given in Tables 1 and 2.

As shown in Fig. 4, halide anions X^- (X = F, Cl, Br) are bound to the amide groups (-NH) on the upper rim of the calix[4]arene *via* the hydrogen bonding (N-H X^-) in

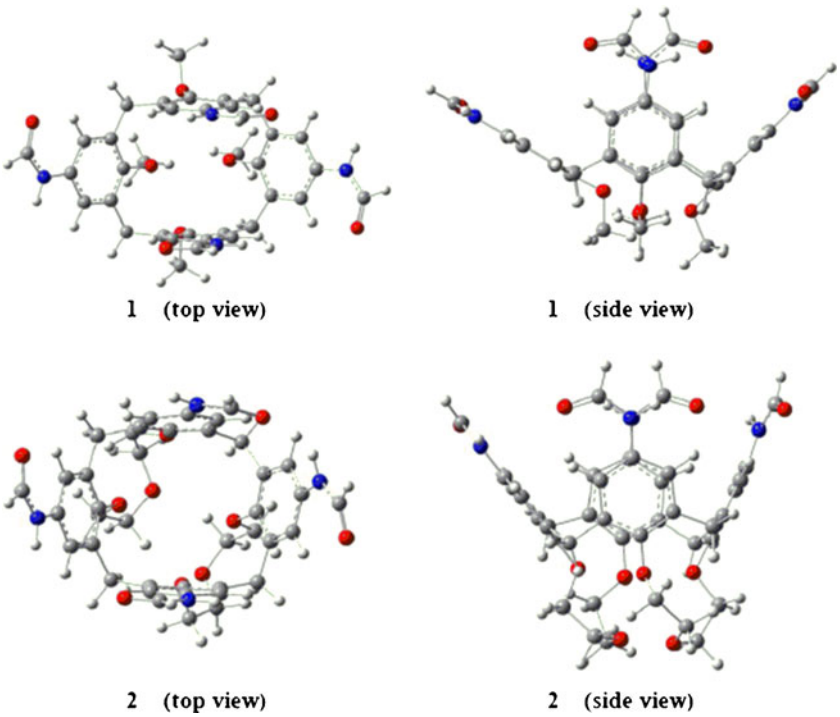

Fig. 2 Optimized structures of **1** and **2** calculated with the B3LYP/LANL2DZp method. The red, blue, deep gray, and shallow gray spheres refer to O, N, C, and H atoms, respectively

Table 1 Selected geometrical parameters of receptor **1** and its complexes M^+X^-/**1** calculated at B3LYP/LANL2DZp level (distance (D) in Å, angle (A) in degree)

Parameters	1	Li^+F^-/1	Na^+F^-/1	K^+F^-/1	Li^+Cl^-/1	Na^+Cl^-/1	K^+Cl^-/1	Li^+Br^-/1	Na^+Br^-/1	K^+Br^-/1
D(N45-H46)	1.015	1.076	1.081	1.078	1.036	1.037	1.038	1.033	1.045	1.046
D(N49-H50)	1.015	1.104	1.080	1.078	1.046	1.037	1.037	1.038	1.016	1.016
D(N45-N49)	5.233	4.671	4.428	4.348	4.930	5.069	4.046	5.464	5.549	5.457
D(N47-N51)	12.105	11.969	10.302	10.045	10.078	10.034	9.990	11.523	9.468	9.281
D(O61-O64)	3.395	3.602	4.467	5.059	3.703	4.485	5.078	3.678	4.525	4.955
D(O62-O63)	5.720	5.200	4.877	5.364	5.220	4.819	5.415	5.001	4.801	5.320
D(O61-O62)	3.499	3.248	3.224	3.581	3.010	3.183	3.696	3.137	3.249	3.484
D(O63-O64)	3.314	3.006	3.224	3.579	3.496	3.190	3.643	2.957	3.188	3.591
D(O61-M^+)		1.878	2.234	2.537	1.914	2.242	2.547	1.890	2.256	2.556
D(O62-M^+)		3.268	2.439	2.699	3.283	2.413	2.752	3.064	2.392	2.708
D(O63-M^+)		2.015	2.440	2.700	1.990	2.406	2.701	1.997	2.413	2.704
D(O64-M^+)		1.876	2.234	2.537	1.894	2.243	2.549	1.887	2.269	2.535
D(H46-X^-)		1.483	1.481	1.492	2.309	2.270	2.249	2.459	2.292	2.280
D(H50-X^-)		1.391	1.484	1.492	2.136	2.270	2.220	2.394	4.347	3.011
A(N45-H46- X^-)		162.1	152.5	150.3	144.1	135.5	157.5	139.4	151.6	151.6
A(N49-H50- X^-)		162.9	152.3	150.3	162.3	135.5	158.4	141.5	98.9	100.1
D(M^+-X^-)		5.963	6.621	7.071	6.411	7.326	7.206	7.076	7.288	6.959
D_{exp}(M^+-X^-)		1.564	1.926	2.172	2.021	2.361	2.667	2.170	2.502	2.821

Table 2 Selected geometrical parameters of receptor **2** and its complexes M^+X^-/**2** calculated at B3LYP/LANL2DZp level (distance (D) in Å, angle (A) in degree)

Parameters	2	Li^+F^-/2	Na^+F^-/2	K^+F^-/2	Li^+Cl^-/2	Na^+Cl^-/2	K^+Cl^-/2	Li^+Br^-/2	Na^+Br^-/2	K^+Br^-/2
D(N45-H46)	1.016	1.084	1.083	1.083	1.037	1.039	1.055	1.041	1.044	1.039
D(N49-H50)	1.015	1.082	1.082	1.082	1.040	1.038	1.015	1.019	1.016	1.021
D(N45-N49)	6.957	4.569	4.526	4.469	5.300	5.191	5.263	5.693	5.690	5.499
D(N47-N51)	10.038	10.450	10.334	10.303	10.157	10.070	9.616	9.860	9.572	9.796
D(O61-O64)	4.109	4.201	4.559	5.019	4.181	4.553	5.046	4.175	4.574	5.012
D(O62-O63)	5.408	4.367	4.628	5.008	4.386	4.625	5.050	4.393	4.631	5.015
D(O61-O62)	3.121	2.924	3.081	3.188	2.919	3.060	3.276	2.927	3.110	3.187
D(O63-O64)	2.941	2.976	3.098	3.198	2.964	3.090	3.210	2.953	3.087	3.177
D(O83-O90)	3.433	2.911	3.455	4.614	2.889	3.426	4.516	2.882	3.384	4.549
D(O61-M^+)		2.185	2.343	2.619	2.172	2.338	2.614	2.158	2.340	2.614
D(O62-M^+)		2.256	2.420	2.681	2.295	2.421	2.668	2.231	2.407	2.670
D(O63-M^+)		2.201	2.332	2.597	2.184	2.325	2.594	2.241	2.331	2.594
D(O64-M^+)		2.078	2.301	2.583	2.081	2.303	2.587	2.081	2.315	2.583
D(O83-M^+)		2.141	2.406	2.678	2.144	2.399	2.662	2.129	2.391	2.664
D(O90-M^+)		2.616	2.583	2.849	2.560	2.580	2.849	2.633	2.577	2.840
D(H46-X^-)		1.472	1.475	1.476	2.276	2.246	2.054	2.357	2.374	2.374
D(H46-X^-)		1.483	1.483	1.480	2.221	2.264	2.834	2.884	2.999	2.999
A(N45-H46- X^-)		155.6	154.5	154.1	136.7	138.3	156.8	145.2	142.8	142.8
A(N49-H50- X^-)		155.0	154.0	153.9	140.2	137.1	96.8	107.2	112.0	112.0
D(M^+-X^-)		6.931	7.099	7.461	7.559	7.757	7.737	7.641	7.738	8.239
D_{exp}(M^+-X^-)		1.564	1.926	2.172	2.021	2.361	2.667	2.170	2.502	2.821

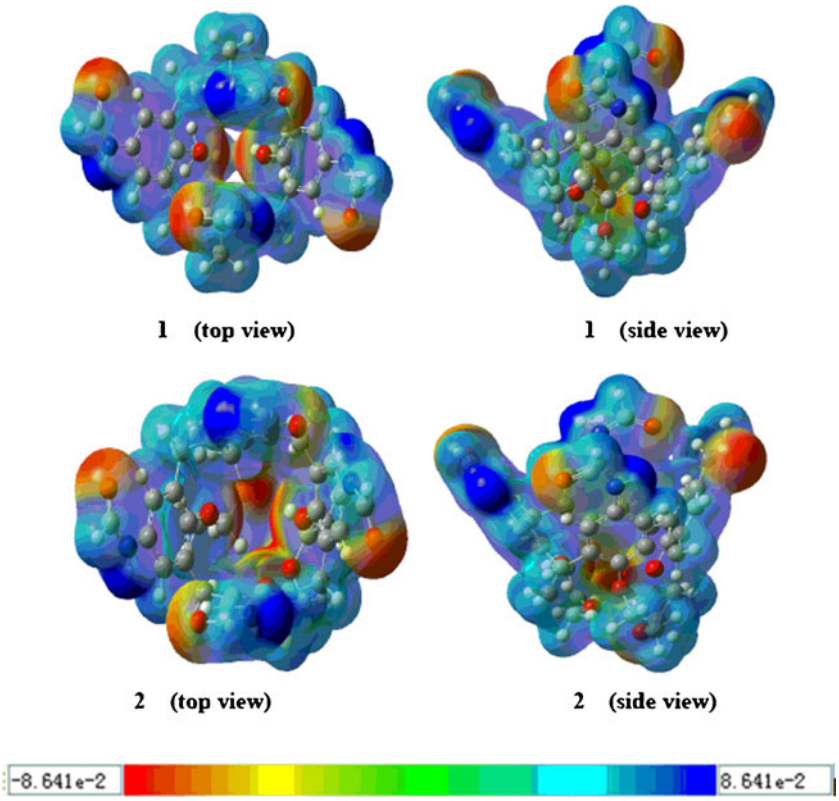

Fig. 3 Plots of the molecular electronic potential presented of receptors **1** and **2**

complexes M^+X^-/H, whereas the alkali cations M^+ (X=Li, Na, K) are complexed by the phenoxy groups (for receptor **1**) or the crown ether components (for receptor **2**) at the lower rim of the calix[4]arene subunit. This result confirmed the MEP prediction. On this basis, the ditopic receptors **1** and **2** bound M^+X^- as an ion-pair, wherein the constituent ions are spatially separated by the host molecule.

As can be seen from Fig. 4, the upper segments in the fully optimized complexes M^+X^-/**1** and M^+X^-/**2** are similar to each other with several N-H X^- hydrogen bonds being involved. The receptor **1** or **2** acts as proton-donor, in which two opposite N-H bonds (N45-H46 and N49-H50) provide protons to each halide anions X^-. It leads to the formation of the intermolecular N-H X^- hydrogen bonds. Furthermore, the other two intramolecular hydrogen bonds (N47-H48 O58 and N51-H52 O60) formed with the decreased distance of H48-O58 and H52-O60 resulting from the inductive effect of anions X^-. All these hydrogen bonds enhance the stability of the resulting complexes. However, due to the different ionic radii and electronegativity of the three halide anions: F^-, Cl^-, and Br^-, the calculated geometrical structures of the inclusion complexes have many differences.

Inspection of Fig. 4 and Tables 1 and 2, shows the intermolecular distances of H46 F^- in Li^+F^-/**1**, Na^+F^-/**1**, and K^+F^-/**1** are 1.483, 1.481, and 1.492 Å, respectively. The angles N45-H46 F^- in three complexes are 162.1, 152.5, and 150.3°, respectively. The distance differences between H50 F^- and H46-F^- in three complexes are small as well as the angle differences. Compared with the free receptors **1** and **2**, the N45-H46 and N49-H50 bond lengths are all elongated more than 0.06 Å after the formation of the inclusion complex M^+F^-/**1** and M^+F^-/**2**, respectively, showing the strong N-H F^- hydrogen bonds. The intramolecular hydrogen bonds (N47-H48 O58 and N51-H52 O60) also existed in complexes M^+Cl^-/H and M^+Br^-/H (H=**1** and **2**). However, there are significant differences between hydrogen bonds N-H Cl^- and N-H Br^- in these corresponding complexes. As to M^+Cl^-/**1**, the distances of H46 Cl^- and H50 Cl^- are 2.309 and 2.136 Å in Li^+Cl^-/**1**, 2.270 and 2.270 Å in Na^+Cl^-/**1**, and 2.249 and 2.220 Å in K^+Cl^-/**1**, respectively. The N45-H46 Cl^- and N49-H50 Cl^- bond angles in above three complexes are 144.1 and 162.3°, 135.5 and 135.5°, and 157.5 and 158.4°, respectively. As to M^+Br^-/**1** (M=Li, Na, K), the corresponding H46 Br^- and H50 Br^- bond lengths are 2.459 and 2.394, 2.292 and 4.347, 2.280 and 3.011 Å, and the N45-H46 Br^- and N49-H50 Br^- bond angles are 139.4 and 141.5, 151.6 and 98.9, 151.6 and 100.1°, respectively. It is clear that either the distances of H X^- or the angles N-H X^-, the hydrogen bonding interactions N-H Br^- are weaker in complexes M^+Br^-/**1** than in M^+Cl^-/**1**. The same results are found for complexes M^+Cl^-/**2** and M^+Br^-/**2**. What's more, compared with the free receptors **1** and **2**, the lengths of N45-H46 and N49-H50 bond lengths in M^+Cl^-/H and M^+Br^-/H are elongated less than 0.04 Å (Tables 1 and 2). All of the above

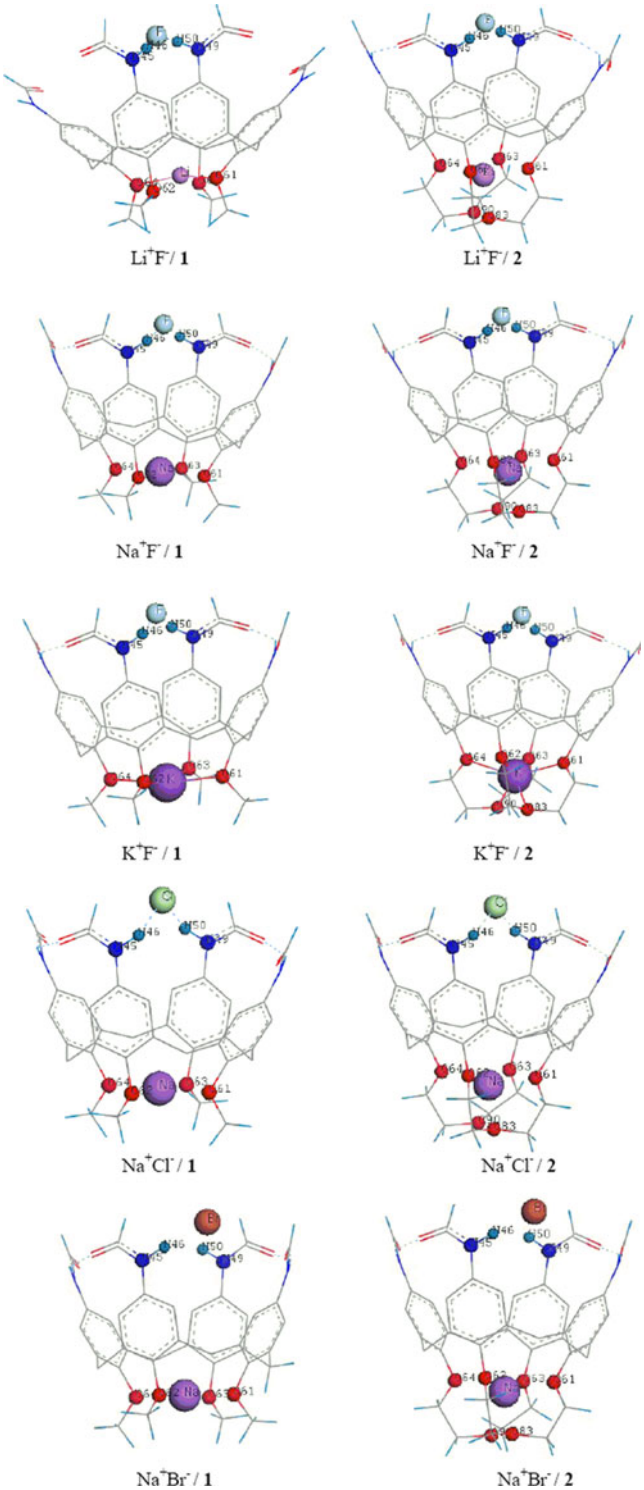

Fig. 4 The structure (side view) of complex M^+X^-/H optimized at the B3LYP/LANL2DZp level with hydrogen bonds ($d_{H\cdots X^-}$<2.5 Å) in dashed blue lines

suggests that the order of the interactions between halide anions and receptors is $F^->Cl^->Br^-$, which is in line with the electronegativity order of halogens.

As shown in Fig. 4 and Tables 1 and 2, the lower segments in the optimized complexes M^+X^-/**1** and M^+X^-/**2** are significantly different due to the differences of the corresponding free receptors **1** and **2**. It is clear that the distances of O61-O64 increase which results in the distances of N47-N51 decrease after the free receptors **1** and **2** coordinating with the ion pairs. What's more, the distances of O62-O64 are all decreased in complexes compared with the free receptors.

In complex Li^+F^-/**1**, the interatomic distances between Li^+-(O61 ~ O64) are 1.878, 3.268, 2.015, and 1.876 Å, respectively. It is clear that the D(Li^+-O62) is much larger than the other three D(Li^+-O). That's to say, Li^+ does not locate in the center of the narrow lower rim surround by the four phenolic oxygens. Similar results are found in complexes Li^+Cl^-/**1** and Li^+Br^-/**1**. However, in complexes Na^+X^-/**1** and K^+X^-/**1** (X = F, Cl, Br), the distances between M^+ (M = Na and K) and O61 ~ O64 are close to each other. It is indicated that Na^+ or K^+ is trapped in the center composed of four phenolic oxygens by metal-oxygen electrostatic interactions. The average distance D(Na^+-O) in complex Na^+F^-/**1** is 2.337 Å, and D(K^+-O) 2.618 Å in K^+F^-/**1**. The binding selectivity often associates with the ionic radius of the alkali cation and the cavity it will occupy. According to the lock-and-key complementarity rule [28], Li^+ is too small to coordinate with all the electron donating oxygen atoms. Even so, the short interatomic distances for Li^+-(O61, O63, O64) indicate the strong interactions between host and guest for isolated molecules in gas phase. In complex Li^+F^-/**2**, the interatomic distances between Li^+-(O61 ~ O64) are 2.185, 2.256, 2.201, and 2.078 Å, respectively, which are slightly longer than the corresponding distances in complex Li^+F^-/**1** except for D(Li^+-O62). However, two further Li^+ binding sites exist in complex Li^+F^-/**2**, namely, O83 and O90. The distances of Li^+-O83 and Li^+-O90 are 2.141 and 2.616 Å. Therefore, Li^+ is trapped in a cavity composed of phenolic oxygens and ether oxygens by metal-oxygen electrostatic interactions. The interatomic distance of O83-O90 decreases by 0.522 Å after the free receptor **2** coordinating with Li^+F^- resulting from the inductive effect of Li^+ O interactions. It reveals that the receptor **2** has to undergo considerable folding/twisting to bring the binding sites into close proximity with the cation. As to complexes Na^+F^-/**2** and K^+F^-/**2**, the distances of O83-O90 are 3.455 and 4.614 Å, respectively, according to the size of cations. On this basis, it was proposed that the cations M^+ are bound to the cavity composed of two crown-3 ether segments, and the interactions of alkali cations with the receptor **2** are stronger than with **1**. The average interatomic distances for M^+-O in the complexes M^+X^-/**1** and M^+X^-/**2** tend to increase from Li^+ to Na^+ to K^+, which is consistent with a increase of the ionic radius of the alkali cation. It is predicted that the selectivity sequence of receptors **1** and **2** for alkali cations in the order of increasing ionic radius, i.e., $Li^+ > Na^+ > K^+$.

To address the ion-pair recognition properties of receptors **1** and **2** in more detail, we list the experimental distances between M and X atoms in alkali metal halides MX in Tables 1 and 2 [29]. As shown in Tables 1 and 2, all the calculated distances D(M^+-X^-) are twice longer than the experimental values D_{exp}(M^+-X^-). Therefore, the ion-pairing of M^+ and X^- is separated completely in the result complexes. Comparing D(M^+-X^-) in Table 2 with the corresponding values in Table 1, the former is bigger. This reflects the two crown ether segments in receptor **2** could bind cooperatively M^+, and the coordination of atoms O83 and O90 with M^+ could draw down M^+ (Fig. 4). It is predicted that the ability of **2** to bind cation M^+ was stronger than that of **1**.

Binding energies and stabilities

The calculated binding energies (ΔE), enthalpy changes (ΔH), Gibbs free energy changes (ΔG), and entropy changes (ΔS) of the result complexes M^+X^-/H based on the Eqs. 2 and 3 at the B3LYP/LANL2DZp level are listed in Table 3.

Table 3 The binding energies ΔE (with ZPE and BSSE correction, kJ mol^{-1}), enthalpy change ΔH (kJ mol^{-1}), Gibbs free energy change ΔG (kJ mol^{-1}), and entropy change ΔS (J $(mol{\cdot}K)^{-1}$) of the complexation reaction at 298 K

Complex	E_{bsse}	ΔE	ΔH	ΔG	ΔS
Li^+F^-/**1**	103.41	−905.56	−1012.18	−926.73	−286.73
Na^+F^-/**1**	104.99	−778.55	−891.18	−800.63	−303.87
K^+F^-/**1**	105.23	−668.57	−780.81	−692.24	−297.12
Li^+Cl^-/**1**	71.56	−771.49	−848.36	−775.58	−244.22
Na^+Cl^-/**1**	60.12	−662.54	−728.81	−641.72	−292.28
K^+Cl^-/**1**	70.43	−589.55	−664.62	−582.94	−273.82
Li^+Br^-/**1**	40.52	−748.91	−794.52	−721.84	−243.88
Na^+Br^-/**1**	45.62	−632.15	−683.24	−597.46	−287.84
K^+Br^-/**1**	48.46	−512.41	−565.15	−483.35	−274.50
Li^+F^-/**2**	110.45	−968.73	−1087.66	−1002.27	−286.55
Na^+F^-/**2**	108.28	−860.98	−976.82	−889.24	−293.87
K^+F^-/**2**	108.25	−731.94	−847.04	−759.81	−292.72
Li^+Cl^-/**2**	66.02	−856.20	−929.34	−847.05	−276.15
Na^+Cl^-/**2**	63.58	−748.36	−818.04	−733.72	−282.95
K^+Cl^-/**2**	72.00	−605.60	−682.67	−600.27	−276.51
Li^+Br^-/**2**	47.97	−827.03	−883.55	−796.20	−293.14
Na^+Br^-/**2**	47.99	−717.36	−770.32	−707.53	−210.72
K^+Br^-/**2**	45.05	−587.60	−639.35	−550.51	−298.12

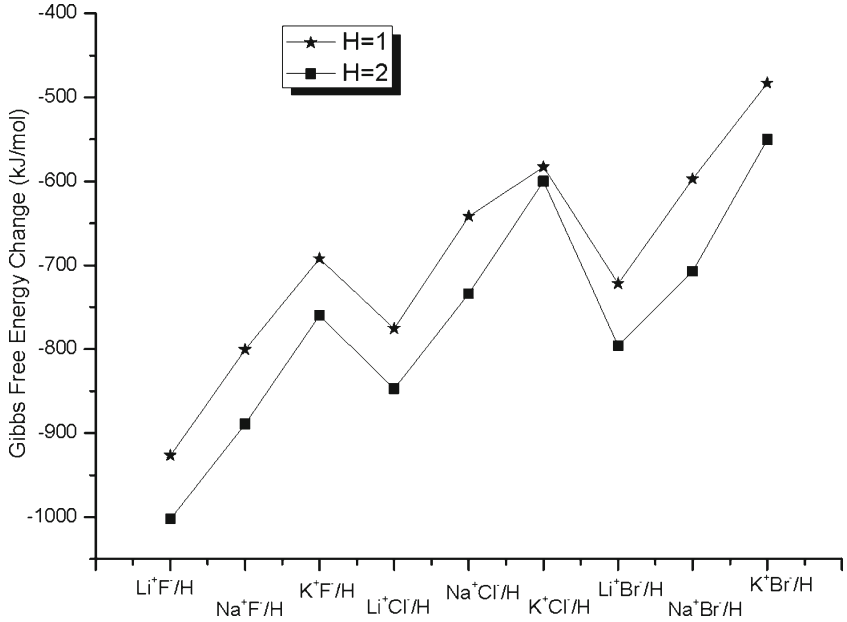

Fig. 5 Change in Gibbs free energy for the complexes M^+X^-/H (M = Li, Na, K; X = F, Cl, Br; H=1, 2.) calculated at B3LYP/LANL2DZp level

As can be seen from Table 3, the calculated binding energies (ΔE) of the complexes M^+X^-/H show the order like that: $\Delta E_{M^+F^-/H} \Delta E_{M^+Cl^-/H} \Delta E_{M^+Br^-/H}$ (for the same cation M^+). This is attributed to the different properties of the three halide anions: F^-, Cl^-, and Br^-. The higher the eletronegativity and the smaller the size of the halogen atom, the stronger the hydrogen bond. Therefore, compared to M^+Cl^-/H, the complexes M^+F^-/H are much easier to exist. However, due to the relatively lower electron density on anion Br^-, the interaction between Br^- and HN- groups is comparatively weak. On the other hand, the calculated ΔE for the two receptors **1** and **2** increases as the alkali cations' size, i.e., $\Delta E_{Li^+X^-/H} \Delta E_{Na^+X^-/H} \Delta E_{K^+X^-/H}$ (for the same anion X^-). Based on the above discussions, both the receptors **1** and **2** show more selectivity toward Li^+F^- and less selectivity toward K^+Br^- among the considered ion pairs M^+X^-. In addition, the negative value of entropy change, ΔS, suggested that the entropy decreased during the complexation process. The high negative values of the Gibbs free energy changes and enthalpy changes, ΔG and ΔH, indicated spontaneous and exothermic nature of the recognition process. Therefore, the inclusion behavior of ion pairs M^+X^- with receptors **1** and **2** were driven by enthalpy under the calculation condition.

Figure 5 shows the Gibbs free energy change of the complexation reactions (1), where we can compare the selectivity of receptors **1** and **2** toward ion pairs M^+X^-. The ΔG results show the same order for all M^+X^-, that is, $\Delta G_{M^+X^-/2} \Delta G_{M^+X^-/1}$ (the M^+X^- in $M^+X^-/2$ is the same as that in $M^+X^-/1$). Therefore, the receptor selectivity of **2** toward the considered ion pairs is higher than that of **1** at the same condition. The selectivity difference between receptors **1** and **2** mainly comes from the different structural feature. In receptor **2**, two crown-3 ether segments on the lower rim of calix[4]arene can form a flexible cavity and have more recognition sites for cations M^+. Therefore, receptor **2** can interact with M^+ more effectively than **1**, though the strength of interaction with anions X^- is similar to each other.

Conclusions

The fully optimized structures of the receptors **1**, **2**, and their complexes with ion pairs M^+X^- (M = Li, Na, K; X = F, Cl, Br) have been obtained at B3LYP/LANL2DZp level in the gas phase. The calculation results indicated that the ion pair receptors **1** and **2** can bind M^+X^- with a 1:1 stoichiometry, and in the complexes the constituent ions are spatially separated by the receptor molecule. Both **1** and **2** can interact with alkali metal cations M^+ *via* the oxygen atoms at the lower rim of the calix[4]arene, while forming hydrogen bonding interaction between the anion X^- and the formylamino groups on the upper rim of the calix[4]arene. From the energetic point of view, the very high stability of the complexes M^+X^-/H reflect the strong interactions between the host and guest molecules, which rest not only on the arrangement of the binding sites but also on the intrinsic properties of the alkali metal cations and the halide anions. The receptor selectivity of **2** toward the considered ion pairs is higher than that of **1**. This study contributes to understand the driving forces and binding sites for the complexation of formylaminocalix[4]arene and formylaminocalix[4]biscrown-3 with ion pairs and provides insights into the host design for ion-pair recognition.

In addition, the solvent effect plays an important role in the stabilization of a particular conformation. Generally speaking, the most favorable structure in the gas phase may not be the most preferred one in solution. Studies of the ion-pair recognition properties in various solution are currently underway in our research group.

Acknowledgments The authors acknowledge the financial support from the Priority Academic Program Development of Jiangsu Higher Education Institutions and the National Natural Science Foundation of China (Grant No. 21103147), China Postdoctoral Science Foundation (20080431123) and Jiangsu Planned Projects for Postdoctoral Research Foundation (0801020 C).

References

1. Kim SK, Sessler JL (2010) Chem Soc Rev 39:3784–3809
2. Ikeda A, Shinkai S (1997) Chem Rev 97:1713–1734
3. Antonisse MMG, Reinhoudt DN (1998) Chem Commun 4:443–448
4. Beer PD, Gale PA (2001) Angew Chem Int Ed 40:486–516
5. Kirkovits GJ, Shriver JA, Gale PA, Sessler JL (2001) J Incl Phenom Macrocycl Chem 41:69–75
6. Martínez-Máñez R, Sancenán F (2003) Chem Rev 103:4419–4476
7. Gokel GW, Leevy WM, Weber ME (2004) Chem Rev 104:2723–2750
8. Gale PA, Quesada R (2006) Coord Chem Rev 250:3219–3244
9. Kim JS, Quang DT (2007) Chem Rev 107:3780–3799
10. Gale PA, Gareía-Garrido SE, Garric J (2008) Chem Soc Rev 37:151–190
11. Caltagirone C, Gale PA (2009) Chem Soc Rev 38:520–563
12. Pescatori L, Arduini A, Pochini A, Secchi A, Massera C, Ugozzoli F (2009) Org Biomol Chem 7:3698–3708
13. Cannizzaro CE, Houk KN (2002) J Am Chem Soc 124:7163–7169
14. Vivas-Reyes R, De Proft F, Biesemans M, Willem R, Geerlings P (2003) Eur J Inorg Chem 6:1315–1318
15. Bernier N, Carvalho S, Li F, Delgado R, Felix V (2009) J Org Chem 74:4819–4827
16. Fennell CJ, Bizjak A, Vlachy V, Dill KA (2009) J Phys Chem B 113:6782–6791
17. Zheng X, Wang X, Yi S, Wang N, Peng Y (2010) J Comput Chem 31:1458–1468
18. Becke AD (1993) J Chem Phys 98:5648–5652
19. Lee C, Yang W, Parr RG (1988) Phys Rev B 37:785–789
20. Hay PJ, Wadt WR (1985) J Chem Phys 82:299–310
21. Dunning TH Jr, Hay PJ, Schaefer HF (1976) Modern Theoretical ChemistryPlenum. New York 3:1-28
22. Huzinaga S, Anzelm J, Klobukowski M, Radzio-Andzelm E, Sakai Y, Tatewaki H (1984) Gaussian basis sets of molecular calculations. Elsevier, Amsterdam
23. Boys SF, Bernardi F (1970) Mol Phys 19:553–566
24. Frisch MJ, Trucks GW, Schlegel HB, Scuseria GE, Robb MA, Cheeseman JR, Scalmani G, Barone V, Mennucci B, Petersson GA, Nakatsuji H, Caricato M, Li X, Hratchian HP, Izmaylov AF, Bloino J, Zheng G, Sonnenberg JL, Hada M, Ehara M, Toyota K, Fukuda R, Hasegawa J, Ishida M, Nakajima T, Honda Y, Kitao O, Nakai H, Vreven T, Montgomery JA, Peralta JE Jr, Ogliaro F, Bearpark M, Heyd JJ, Brothers E, Kudin KN, Staroverov VN, Keith T, Kobayashi R, Normand J, Raghavachari K, Rendell A, Burant JC, Iyengar SS, Tomasi J, Cossi M, Rega N, Millam JM, Klene M, Knox JE, Cross JB, Bakken V, Adamo C, Jaramillo J, Gomperts R, Stratmann RE, Yazyev O, Austin AJ, Cammi R, Pomelli C, Ochterski JW, Martin RL, Morokuma K, Zakrzewski VG, Voth GA, Salvador P, Dannenberg JJ, Dapprich S, Daniels AD, Farkas O, Foresman JB, Ortiz JV, Cioslowski J, Fox DJ (2010) Gaussian 09, Revision B.01. Gaussian Inc, Wallingford
25. Cramer CJ (2002) Essentials of Computational Chemistry: Theories and Models. Willy, West Sussex
26. Shinkai S, Masato I, Sugasaki A, Masayuki T (2001) Acc Chem Res 34:494–503
27. Roy DK, Balanarayan P, Gadre SR (2009) J Chem Sci 121:815–821
28. Pedersen C (1970) J Am Chem Soc 92:391–394
29. Lide DR (2003-2004) CRC handbook of chemistry and physics, 84th ed. CRC, Boca Raton, (9):19-20